J. Fluid Mech. (1999), *vol.* 385, *pp.* 359–379. Printed in the United Kingdom

Hydrodynamic and boundary-layer dispersion in bidisperse porous media

By KONSTADINOS N. MOUTSOPOULOS[1] AND DONALD L. KOCH[2]

[1]Laboratory of Mechanics and Material Science, Laboratory of Rural Engineering, Engineering School, Aristotle University of Thessaloniki, 54006 Thessaloniki, Greece

[2]School of Chemical Engineering, Cornell University, Ithaca, NY 14853, USA

(Received 26 September 1997 and in revised form 2 December 1998)

The small grains in a bidisperse porous medium have the greater influence on the permeability, while the large grains are more effective in dispersing chemical tracers. We compute the dispersion induced by a dilute array of large spheres in a Brinkman medium whose permeability is determined by the radii and volume fraction of the small spheres. The effective diffusivity contains a purely hydrodynamic contribution proportional to $Ua_1\phi_1$ and an $O(Ua_1\phi_1 \ln(Ua_1/D))$ contribution from the mass transfer boundary layers near the spheres. Here, U is the mean velocity in the medium, a_1 and ϕ_1 are the radii and volume fraction of the large spheres and D is the molecular diffusivity. The boundary-layer dispersion is small when the Brinkman screening length κ (or square root of permeability) is much smaller than a_1, but is important for $\kappa \geqslant O(a_1)$. Experimental results for the dispersion due to flow through a bidisperse packed bed are reported and compared with the theoretical predictions. In addition to its application to bidisperse porous media, the present calculation allows an extension of Koch & Brady's (1985) analysis of monodisperse fixed beds to include higher-order terms in the expansion for small particle volume fraction.

1. Introduction

The dispersion of heat and mass plays an important role in a variety of applications including the transport of pollutants in aquifers, extraction of geothermal energy, interseasonal storage of heat, secondary oil recovery, transport of fertilizers, mechanisms for the alteration of certain types of geological formations and the design of packed-bed reactors. When the Péclet number $Pe = Ua_1/D$ is much larger than one, the effective diffusivity produced by a mean fluid velocity U through a porous medium with a characteristic length scale a_1 is much larger than the molecular diffusivity D. The simple assumption that the dispersion is purely mechanical and independent of the molecular diffusivity leads to an effective diffusivity proportional to Ua_1. However, Saffman (1959) and Koch & Brady (1985) showed that a contribution to the effective diffusivity that is proportional to $Ua_1 \ln(Pe)$ results from tracers that come close to no-slip solid boundaries in the medium; these tracers could not escape the slow-moving region near the boundary without the aid of molecular diffusion.

Porous media are often modelled as either an array of pores (Salles *et al.* 1993; Koplik, Redner & Wilkinson 1988; Sahimi & Imdakm 1988) in a continuous solid matrix or as an array of fixed spherical particles or grains in a continuous fluid phase (Brenner 1980; Eidsath *et al.* 1983; Koch & Brady 1985). While the former model

more closely approximates many consolidated porous rocks, the latter is appropriate for sandy soils and packed-bed reactors. The modelling of dispersion in pore networks requires an arbitrary assumption that the fluid in the nodes between pores is well mixed whereas no such assumption is required for the fixed-bed model.

Koch & Brady (1985) derived the effective diffusivity in a dilute, monodisperse fixed bed of spherical particles. The effect of the surrounding particles on the conditionally averaged velocity caused by a test particle was modelled in terms of a body force in Brinkman's momentum equation with a permeability $\kappa^2 = (2/9)a_1^2/\phi_1$. In the dilute limit with the volume fraction $\phi_1 \ll 1$, the Brinkman screening length $\kappa \gg a_1$. Since the leading contribution to the dispersion came form $O(\kappa)$ radial separations from the test particle, Koch & Brady exploited the point-particle approximation for the fluid velocity disturbance induced by the particle. This led to a mechanical contribution $(27/8)U\phi_1\kappa^2/a_1 = (3/4)Ua_1$ to the effective diffusivity. Koch & Brady noted that the dispersion was not entirely independent of molecular diffusivity. The no-slip boundary condition on the solid sphere leads to a contribution $(\pi^2/6)Ua_1\phi_1 \ln(Pe)$ to the effective diffusivity that arises from the mass transfer boundary layer of thickness $\delta = O(a_1 Pe^{-1/3})$ near the particle surface. This leading-order boundary-layer contribution was determined by scaling the mass conservation equation in the boundary layer and without obtaining a full solution to the boundary-layer equations. Terms of order $Ua_1\phi_1^{1/2}$ and $Ua_1\phi_1$ neglected in Koch & Brady's analysis can only be determined from a complete solution of the conditionally averaged concentration field surrounding a finite radius particle. Such a solution is undertaken in this paper.

In addition to the dispersion caused by individual grains, field-scale measurements in heterogeneous porous media are typically influenced by spatial variations in permeability and by macroscopic impermeable inclusions. A number of researchers including Smith & Schwartz (1980), Koch & Brady (1988), and Lenormand & Wang (1995) have investigated the dispersion resulting from macroscopic variations in permeability. Moutsopoulos & Bories (1993) studied dispersion in a medium consisting of a porous matrix satisfying Darcy's equations of motion with impermeable spherical inclusions. These inclusions could represent small soil cores of gravel or larger scale impermeable regions such as clay lenses. These types of geological formations often occur in aquifers near rivers and influence the dispersion of pollutants as the river water infiltrates the aquifer. In the present study, we assume that the inclusions are not only impermeable to the flow but impenetrable by the solute. However, this assumption could be relaxed by incorporating a description of the diffusion and mass transfer within the inclusions (see, for example, Koch & Brady 1985).

This paper addresses the dispersion occurring in a bidisperse fixed bed consisting of two species of spheres with volume fractions ϕ_1 and ϕ_2 and radii a_1 and a_2 with $a_1 > a_2$. This could model a medium consisting of grains of differing sizes. Alternatively, the large spheres could represent large-scale impermeable regions as suggested by Moutsopoulos & Bories (1993). The permeability of the medium is usually controlled primarily by the smaller particles. For example, when $\phi_1 \ll 1$, the overall permeability of the bidisperse medium is $k = k_2(1 - 3\phi_1/2)$, where k_2 is the permeability of a monodisperse medium of small particles with radius a_2 and volume fraction $\phi_2/(1 - \phi_1)$. On the other hand, large grains lead to larger displacements of tracers and usually cause more dispersion. Thus, we will consider a model of bidisperse porous media in which the small particles give rise to a porous matrix described by Brinkman's equations of motion and the hydrodynamic dispersion is enhanced by the fluid flow around the large obstacles of radius a_1 embedded in this medium. The use of Brinkman's equations to describe the conditionally averaged velocity field around

a large inclusion allows us to capture the boundary-layer dispersion that arises near the no-slip solid boundary to the large sphere; this effect would be missed if one used Darcy's equations of motion.

In § 2, we consider media with moderate to small permeabilities $\kappa \leqslant O(a_1)$ where $\kappa = k_2^{1/2}$ is the Brinkman screening length. We assume $a_2 \ll a_1$ so that the small particles only serve to produce a Brinkman medium with a permeability k_2 in which the dilute array ($\phi_1 \ll 1$) of larger particles are imbedded. The ensemble-averaged equations are introduced in § 2.1 and the hydrodynamic and boundary-layer dispersion are computed in §§ 2.2 and 2.3, respectively. The use of Brinkman's equations to describe the conditional-average velocity around a large sphere can be justified rigorously when $\phi_2 \ll 1$. This limit is compatible with moderate permeabilities $\kappa \sim O(a_1)$ provided that $a_2/a_1 = O(\phi_2^{1/2}) \ll 1$. In § 3, we consider highly permeable arrays $\kappa \gg a_1$ with no restriction on the size ratio a_1/a_2. In the case $\phi_2 = 0$, the results of § 3 provide a higher-order approximation for the dispersion in a monodisperse dilute array that improves upon the theory of Koch & Brady (1985). Experimental measurements of dispersion in bidisperse packed beds are presented and compared with the theoretical predictions in § 4. This comparison indicates that the qualitative predictions of enhanced dispersion due to the incorporation of large spheres into a packed bed of small spheres are valid even in concentrated packed beds, $\phi_2 \sim O(1)$.

2. Theory for moderate permeabilities $\kappa \leqslant O(a_1)$

2.1. *Governing equations*

In this section, we consider a model of a bidisperse porous medium in which it is assumed that the small grains only affect the medium by contributing a permeability k_2. Thus, the medium consists of a dilute array of impermeable spherical inclusions of volume fraction ϕ_1 and radii a_1 embedded in a medium described by Brinkman's (1947) equations of motion:

$$\nabla \cdot \boldsymbol{u} = 0, \tag{1}$$

$$-\mu \nabla^2 \boldsymbol{u} + \nabla p + \frac{\mu}{k_2} \boldsymbol{u} = 0, \tag{2}$$

where μ is the fluid viscosity and p the fluid pressure. Brinkman's equations can be derived by ensemble averaging the equations of motion over all possible configurations of the small (species 2) particles leading to equations of the form (1) and (2) in the limit $\phi_2 \ll 1$ (Hinch 1977). Here, $\boldsymbol{u}$ is the mean velocity in the Brinkman medium ensemble averaged over the possible configurations of the small particles compatible with a given large particle structure. The fluid velocity satisfies a no-slip boundary condition $\boldsymbol{u} = \boldsymbol{0}$ at the surfaces of the large particles and the mean value $\langle \boldsymbol{u} \rangle = \boldsymbol{U}$ is independent of position and time. The angle brackets indicate an ensemble average over all possible configurations of the large spheres.

In the dilute limit $\phi_1(\kappa/a_1)^3 \ll 1$, most of the particles of species 2 will be separated from all 1-particles by a sufficient distance r (where $r \gg \kappa$) so that they are unaffected by the larger particles. Thus, the dispersion caused by the particles of species 2 can be obtained from monodisperse dispersion theory (Koch & Brady 1985); this dispersion will be $O(Ua_2)$ for both $\phi_2 = O(1)$ and $\phi_2 \ll 1$. We will focus attention on the $O(Ua_1\phi_1)$ dispersion that arises due to the large particles. The large particles make the dominant contribution to the effective diffusivity provided that the size ratio is

sufficiently large $a_1/a_2 \gg 1/\phi_1$. This condition is compatible with any value of κ/a_1 because κ may be adjusted by varying ϕ_2.

The conservation equation for the tracer is

$$\frac{\partial c}{\partial t} + \nabla \cdot (\boldsymbol{v}c) - D\nabla^2 c = 0. \tag{3}$$

Here, c is the concentration of the tracer ensemble averaged over the configurations of small particles. The particles are impermeable to the tracer so the tracer velocity $\boldsymbol{v} = \boldsymbol{u}/(1-\phi_2)$ is larger than the mean velocity $\boldsymbol{u}$ of the medium. The third term on the left-hand side of (3) represents the dispersion of the tracer. We are interested in the dispersion that occurs at high Péclet numbers, $Pe = Ua_1/D \gg 1$, and in this limit molecular diffusion is small compared with convection in the bulk of the medium. Furthermore, we are interested in situations in which the length scale of the flow, which is $l = \max[a_1, \kappa]$, is much larger than the radii of the small spheres a_2. Since the effective diffusivity due to the small spheres is $D_{eff} = O(Ua_2)$, a Péclet number, $Pe_{eff} = Ua_1/D_{eff} = O(l/a_2)$ is also large and the hydrodynamic dispersion caused by the small spheres is small compared with convection. The diffusion term in (3) is only important in a thin boundary layer near the surface of the large spheres where the convective velocity approaches zero. Koch (1966) showed that the hydrodynamic diffusion becomes small and molecular diffusion dominates within this boundary layer. Therefore, we have incorporated only the molecular diffusivity D in equation (3). The applicability of this approximation will be discussed further at the end of § 2.3.

It will be assumed that the tracer cannot penetrate the spheres so that the concentration field satisfies a no-flux boundary condition $\boldsymbol{n} \cdot \nabla c = 0$ at the surfaces of the large particles. Adsorption or absorption within the spheres could be incorporated into the model and would lead to an additional mechanism of dispersion as discussed by Koch & Brady (1985).

Taking the ensemble average of (3) and assuming that the Péclet number $Pe = Ua_1/D$ is very large (so that the molecular diffusion term in (3) is small) leads to an equation for the average concentration field:

$$\frac{\partial \langle c \rangle}{\partial t} + \boldsymbol{W} \cdot \nabla \langle c \rangle - \nabla \cdot (\boldsymbol{D}^* \cdot \nabla \langle c \rangle) = 0, \tag{4}$$

where

$$\boldsymbol{W} = \boldsymbol{U}/(1 - \phi_1 - \phi_2) \tag{5}$$

is the average velocity of the fluid and therefore also the averge velocity of the fluid phase tracer and $\boldsymbol{D}^*$ is the effective diffusivity, which is given by

$$-\boldsymbol{D}^* \cdot \nabla \langle c \rangle = \langle \boldsymbol{v}' c' \rangle = n \int \mathrm{d}\boldsymbol{x}_1 \langle \boldsymbol{v}' c' \rangle_1 \approx n \int \mathrm{d}\boldsymbol{x}_1 \langle \boldsymbol{v}' \rangle_1 (\boldsymbol{x}|\boldsymbol{x}_1) \langle c' \rangle_1 (\boldsymbol{x}|\boldsymbol{x}_1). \tag{6}$$

Here, $\langle\,\rangle_1$ is the conditional ensemble average with the position of one particle centre held fixed at $\boldsymbol{x}_1$, $\boldsymbol{v}' = \boldsymbol{v} - \boldsymbol{w}$, and $c' = c - \langle c \rangle$. For $k_2^{1/2} \equiv \kappa_2 = O(a_1)$, the relative errors incurred in the final approximation in (6) are $O(\phi_1)$; they grow to $O(\phi_1^{1/2})$ when $\kappa_2 \geqslant O(a\phi_1^{-1/2})$. In many studies of tracers that do not permeate the particles (for example, Fried & Combarnous 1971), the dispersion equation is written for the concentration field $\langle c \rangle^f$ averaged over the fluid phase; this is related to $\langle c \rangle$ (the average over both fluid and particle phases) by $\langle c \rangle^f = \langle c \rangle/(1 - \phi_1 - \phi_2)$ and an equation for $\langle c \rangle^f$ in a homogeneous medium can be obtained by multiplying (4) by $1/(1 - \phi_1 - \phi_2)$.

The local diffusive approximation to the flux assumed in (6) is valid provided that the mean concentration gradient varies sufficiently slowly in space and time. Koch & Brady (1988) have introduced a non-local description of dispersion in the presence of rapidly varying concentration gradients. In the present paper, we will consider only local diffusion and, for covenience, we treat $\nabla\langle c\rangle$ as a constant. A solution to (4) that corresponds to a constant mean concentration gradient throughout an unbounded porous medium is

$$\langle c\rangle = (\boldsymbol{x} - \boldsymbol{W}t)\cdot\nabla\langle c\rangle + c_0, \tag{7}$$

where c_0 is a constant. The dispersion tensor in an isotropic porous medium will take the form

$$\boldsymbol{D}^* = D_L^*\boldsymbol{e}_z\boldsymbol{e}_z + D_T^*(\boldsymbol{I} - \boldsymbol{e}_z\boldsymbol{e}_z), \tag{8}$$

where D_L^* and D_T^* are the longitudinal and transverse dispersivities and z is the coordinate measured parallel to the direction of the mean flow.

Taking the conditional ensemble average of the mass conservation equation and subtracting the bulk average equation (4) gives

$$\frac{\partial\langle c'\rangle_1}{\partial t} + \nabla\cdot[\langle(\boldsymbol{v} - \langle\boldsymbol{v}\rangle_1^f)(c - \langle c\rangle_1)\rangle_1 - \langle\boldsymbol{v}'c'\rangle] + \langle\boldsymbol{v}'\rangle_1^f\cdot\nabla\langle c'\rangle_1 - D\nabla^2\langle c'\rangle_1 = -\langle\boldsymbol{v}'\rangle_1^f\cdot\nabla\langle c\rangle. \tag{9}$$

In this section, we will neglect the term $\nabla\cdot[\langle(\boldsymbol{v} - \langle\boldsymbol{v}\rangle_1^f)(c - \langle c\rangle_1)\rangle_1 - \langle\boldsymbol{v}'c'\rangle]$, which describes the effects of interactions among the large spheres and is $O(\phi_1)$ smaller than the terms retained.

In order to determine the conditionally averaged concentration from (9) and the effective diffusivity from (6), we require an equation for the conditionally averaged fluid velocity in the region surrounding the test sphere. This is obtained by ensemble averaging (1) and (2) to obtain

$$-\mu\nabla^2\langle\boldsymbol{u}\rangle_1 + \nabla\langle p\rangle_1 + \frac{\mu}{k_2}\langle\boldsymbol{u}\rangle_1 = \int_{|\boldsymbol{x}_2-\boldsymbol{x}|=a} \mathrm{d}\boldsymbol{x}_2 P(\boldsymbol{x}_2|\boldsymbol{x}_1)\,\boldsymbol{n}\cdot\langle\boldsymbol{T}\rangle_2(\boldsymbol{x}|\boldsymbol{x}_1,\boldsymbol{x}_2), \tag{10}$$

$$\nabla\cdot\langle\boldsymbol{u}\rangle_1 = 0, \tag{11}$$

where $\langle\boldsymbol{T}\rangle_2$ is the stress tensor conditionally averaged with two particle positions held fixed, $\boldsymbol{n}$ is the unit normal to the second sphere, and $P(\boldsymbol{x}_2|\boldsymbol{x}_1)$ is the conditional average probability density for finding a particle centred at $\boldsymbol{x}_2$ given that the test sphere is centred at $\boldsymbol{x}_1$. The integral on the right-hand side of (10) represents the force per unit volume that other particles of species 1 exert on the fluid surrounding the test particle. This body force is small in a dilute array ($\phi_1 \ll 1$) and it may be neglected whenever $\kappa_2 = O(a_1)$. When $\kappa_2 \gg a_1$, this body force can be approximated as $6\pi\mu a_1 n_1\langle\boldsymbol{u}\rangle_1$ where $n_1 = \phi_1/(4\pi a_1^3/3)$ is the number density of species 1. Thus, (10) may in general be approximated as

$$-\mu\nabla^2\langle\boldsymbol{u}\rangle_1 + \nabla\langle p\rangle_1 + \frac{\mu}{k}\langle\boldsymbol{u}\rangle_1 = 0, \tag{12}$$

where the permeability is approximately that due to species 2 if (as in the present section) the array is moderately permeable,

$$k = k_2 \quad \text{for} \quad k_2^{1/2} \ll a_1\phi_1^{-1/2}, \tag{13}$$

and is given by

$$k^{-1} = k_2^{-1} + \frac{9}{2}\frac{\phi_1}{a_1^2} \quad \text{for} \quad k_2 \gg a_1^2 \quad \text{and} \quad \phi_1 \ll 1 \tag{14}$$

in a highly permeable dilute array. Since the second term in (14) becomes important only when the medium of species 2 spheres has a very high permeability $k_2 \gg a_1^2$, (14) provides a uniformly valid approximation for the permeability.

The solution of (11) and (12) for the conditional-average fluid velocity field outside a fixed sphere is

$$\begin{aligned}\langle \boldsymbol{u} \rangle_1 = \boldsymbol{U} \left(1 + \left(1 + \frac{3\kappa}{a_1} + \frac{3\kappa^2}{a_1^2}\right)\frac{a_1^3}{2r^3} - \frac{3}{2}\left(\frac{a_1}{r} + \frac{\kappa a_1}{r^2} + \frac{\kappa^2 a_1}{r^3}\right)\exp\left(-\frac{r-a_1}{\kappa}\right)\right) \\ -\frac{\boldsymbol{U}\cdot\boldsymbol{r}\boldsymbol{r}}{r^2}\left(\left(1 + \frac{3\kappa}{a_1} + \frac{3\kappa^2}{a_1^2}\right)\frac{3a_1^3}{2r^3} - \frac{3}{2}\left(\frac{a_1}{r} + \frac{3a_1\kappa}{r^2} + \frac{3a_1\kappa^2}{r^3}\right)\exp\left(-\frac{r-a_1}{\kappa}\right)\right),\end{aligned} \tag{15}$$

where $\boldsymbol{r} = \boldsymbol{x} - \boldsymbol{x}_1$ and $\kappa = k^{1/2}$ is the Brinkman screening length. The conditional-average velocity of the tracer in the fluid phase may be obtained using $\langle \boldsymbol{v} \rangle_1^f \approx \langle \boldsymbol{u} \rangle_1/(1 - \phi_1 - \phi_2)$; this relationship has $O(\phi_1)$ errors for $r < 2a_1$ and is exact for $r > 2a_1$.

An important feature of the forthcoming analysis will be the application of Brinkman's averaged equations of motion (11) and (12) and their solution for flow past a sphere (15) at all positions surrounding a fixed large sphere with no-slip boundary conditions. When these equations are derived by volume averaging (Bear 1978; Aifantis 1980), their applicability to separations from the large sphere that are smaller than the typical interparticle spacing of the small particles is unclear. However, the ensemble-averaging derivation demonstrates that Brinkman's equations apply at all separations in a medium that is dilute in both particle species (Hinch 1977; Koch 1996). In general, the permeability may vary in the vicinity of a solid boundary to the medium (such as the surface of a large sphere) as a result of exclusion of particles by the impenetrable wall and hydrodynamic reflections between the particle and the wall; however, the effect of these phenomena on the conditional-average velocity is asymptotically small when $\phi_2 \ll 1$ (Koch 1996). Furthermore, the ensemble-average approach makes it clear that the appropriate boundary condition for the conditional-average velocity at the surface of the fixed particles is a no-slip boundary condition; this results simply from the fact that the velocity is zero for each member of the sub-ensemble in which the point of interest is on the surface of the fixed particle.

Numerical simulations (Durlofsky & Brady 1987) indicate that Brinkman's equations accurately describe the conditional ensemble-average velocity field with one particle position specified in a dilute fixed bed. In more concentrated fixed beds, the predictions of Brinkman's equations for the detailed velocity profile are inaccurate. However, predictions based on Brinkman's equation for averaged properties such as the drag on a particle (Koch & Ladd 1997), the overall dispersion (Koch & Brady 1985) and the slip velocity at the boundary between a porous medium and a pure fluid region (Sangani & Behl 1989) are still reasonably good. More sophisticated models of flow near the boundary of a porous medium that include variations in permeability and viscosity and/or terms involving higher-order derivatives of the velocity field have been proposed (see, for example, Acrivos & Chang 1986; Muthukumar & Freed 1979). Predictions for the dispersion resulting from these models could be obtained using the same general procedure as outlined below for the Brinkman equation.

2.2. *Hydrodynamic diffusion*

It is observed that the effective diffusivities of non-adsorbing tracers in porous media at high Péclet numbers are nearly independent of the molecular diffusivity. An apparent dispersion that is independent of molecular diffusion is referred to as hydrodynamic diffusion. The fore–aft symmetry of the streamlines for Brinkman flow past a sphere imply that there will be no net displacement of a tracer perpendicular to the direction of the mean flow. As a consequence, we will obtain a contribution only to the longitudinal component of the diffusion tensor. This longitudinal diffusivity can be computed by considering an average concentration gradient that is parallel to the flow direction. To look for a hydrodynamic diffusivity, we drop the molecular diffusion term in the equation (9) for the conditionally averaged concentration field and integrate this equation along a streamline to obtain

$$\langle c' \rangle_1 = -\int_{-\infty}^{\eta} \mathrm{d}\eta' \frac{\langle \boldsymbol{v}' \rangle_1^f \cdot \nabla \langle c \rangle}{h_\eta |\langle \boldsymbol{v} \rangle_1^f|}. \tag{16}$$

Here, Φ is the meridional angle, Ψ is the stream function, η is a third orthogonal coordinate that measures distance along a given streamline, and h_η is the associated metric coefficient. Substituting (16) into (6), the longitudinal dispersion coefficient is given by

$$D_L^* = n \int \mathrm{d}\boldsymbol{r} \langle v_z' \rangle_1^f (\Psi, \eta, \Phi) \int_{-\infty}^{\eta} \mathrm{d}\eta' \frac{\langle v_z' \rangle_1^f}{h_\eta |\langle \boldsymbol{v} \rangle_1^f|}. \tag{17}$$

Koch & Brady (1985) simplified (17) by considering a highly permeable array. In this case, the largest contributions to the volume integral came from large separation distances $r \sim O(\kappa) \gg a_1$ and it was thereby possible to use a point-particle approximation for the velocity field (15) and approximate the streamlines as straight lines in the z-direction. Moutsopoulos & Bories (1993) considered the opposite limit of a medium with a very small Brinkman screening length. They derived Ψ and η for the solution to Darcy's equations of motion. For the present case, $\kappa \sim O(a_1)$, we require the stream function corresponding to the Brinkman velocity field (15); this is given by

$$\Psi = \tfrac{1}{2} U \sin^2\theta \left[r^2 - \left(a_1^3 + 3\kappa a_1^2 + 3\kappa^2 a_1\right) \frac{1}{r} + 3\left(\kappa a_1 + \frac{\kappa^2 a_1}{r}\right) \exp\left(-\frac{r - a_1}{\kappa}\right)\right], \tag{18}$$

where r and θ are the radial coordinate and azimuthal angle in a spherical coordinate system whose origin is the centre of the sphere and whose axis is parallel to $\boldsymbol{U}$. Differentiating (18) to obtain a differential equation for $r(\theta)$ along the streamline, using geometry to derive the differential equation for $\theta(r)$ along a line perpendicular to the streamlines and integrating yields the following expression for the orthogonal coordinate:

$$\eta = U \cos\theta \exp\left(\int H(r')\,\mathrm{d}r'\right), \tag{19}$$

where

$$H(r) = \frac{2}{r}\left(\frac{r^3 - (a_1^3 + 3\kappa a_1^2 + 3\kappa^2 a_1) + 3(\kappa r a_1 + \kappa^2 a_1)\exp[-(r - a_1)/\kappa]}{2r^3 + (a_1^3 + 3\kappa a_1^2 + 3\kappa^2 a_1) - 3(r^2 a_1 + \kappa r a_1 + \kappa^2 a_1)\exp[-(r - a_1)/\kappa]}\right). \tag{20}$$

In the limit $\kappa \ll a_1$, (19) reduces to the classical result for the potential lines for Darcy flow or flow of a perfect fluid, i.e. $\eta = U\cos\theta[r + (a_1^3/2r^2)]$. The metric coefficient is

$$h_\eta = \left(H^2\cos^2\theta + \frac{1}{r^2}\sin^2\theta\right)^{1/2} U\exp\left(\int H(r')\,\mathrm{d}r'\right). \tag{21}$$

To compute the longitudinal diffusivity (17), it is most convenient to express the volume integral in terms of the streamline coordinates (Ψ, η, Φ). The integral over Φ can be performed analytically owing to the axisymmetry yielding

$$D^*_{L,H} = \phi_1 Wa_1 J, \tag{22}$$

where

$$J = \frac{3}{2Ua_1^3}\int_{-\infty}^{\infty}\mathrm{d}\eta\int_{\Psi_0(\eta)}^{\infty}\mathrm{d}\Psi\, r^2\sin\theta\left|\frac{\mathrm{D}(\Psi,\eta)}{\mathrm{D}(r,\theta)}\right|^{-1}\langle u_z'\rangle_1(\eta,\Psi)\int_{-\infty}^{\eta}\mathrm{d}\eta'\frac{\langle u_z'\rangle_1}{h_\eta|\langle \boldsymbol{u}\rangle_1|}. \tag{23}$$

The Jacobian in (23) may be computed analytically using (18) and (19), but the resulting expression is long and is omitted for brevity. It is most convenient to express the fluid velocity, the Jacobian and the metric coefficient in terms of the spherical coordinates (r, θ). Thus, to perform the integration in (23) we must obtain the values of r and θ corresponding to a specified point in streamline coordinates (Ψ, η). This was accomplished by combining (18) and (19) to eliminate θ. The resulting nonlinear algebraic equation for r was solved using Newton–Raphson or bisection iterations. The integrals in (23) were performed using the finite element method with grid spacings chosen to achieve a relative error of less than 0.1%.

The tracer dispersion arises from the entire region of fluid surrounding the fixed particle. However, an attempt to perform the integral in (23) over all values of the stream function Ψ from 0 (corresponding to the particle surface) to ∞ (far from the particle) would lead to a logarithmic divergence. The magnitude of the velocity goes to zero at the no-slip solid boundary to the particle and tracer molecules that come close to the particle therefore spend a long time near the surface. This leads to a large contribution to the overall dispersion. Koch & Brady (1985) referred to this phenomenon as boundary-layer dispersion and pointed out that molecular diffusion must play a role in allowing tracer molecules to escape the slow-moving fluid near the particle surface. We have neglected molecular diffusion in the analysis leading to (23) and so we have placed a lower limit of integration $\Psi_0(\eta)$, which corresponds to a radial distance of $y = r - a_1 = \zeta a_1$ from the particle surface. The dispersion arising due to the fluid closer to the particle will be treated in the following subsection through the analysis for boundary-layer dispersion that incorporates the effects of molecular diffusion. The precise value of the radial distance at which we make the transition from the present hydrodynamic diffusion analysis to the subsequent boundary-layer dispersion analysis is unimportant as long as $a_1\zeta$ is large compared with the boundary-layer thickness δ and small compared with a_1. Both analyses are valid in the regime $\delta \ll y \ll a_1$. In practice we used $\zeta = 0.05$ for $\kappa/a_1 \geqslant 1$ and $\zeta = 0.05(\kappa/a_1)$ for $\kappa/a_1 \leqslant 1$.

Results for the longitudinal hydrodynamic diffusivity scaled by $Wa_1\phi_1$ are plotted as a function of κ/a_1 in figures 1 and 2. The scaled dispersivity approaches 0.188, the value obtained for Darcy flow by Moutsopoulous & Bories (1993) as $\kappa/a_1 \to 0$. The dispersivity approaches Koch & Brady's (1985) result $(27/8)\,(\kappa/a_1)^2$ (dashed line) for a highly permeable array as $\kappa/a_1 \to \infty$. However, we note that the approach to this dilute fixed-bed asymptote is rather slow. An improved asymptotic expression for

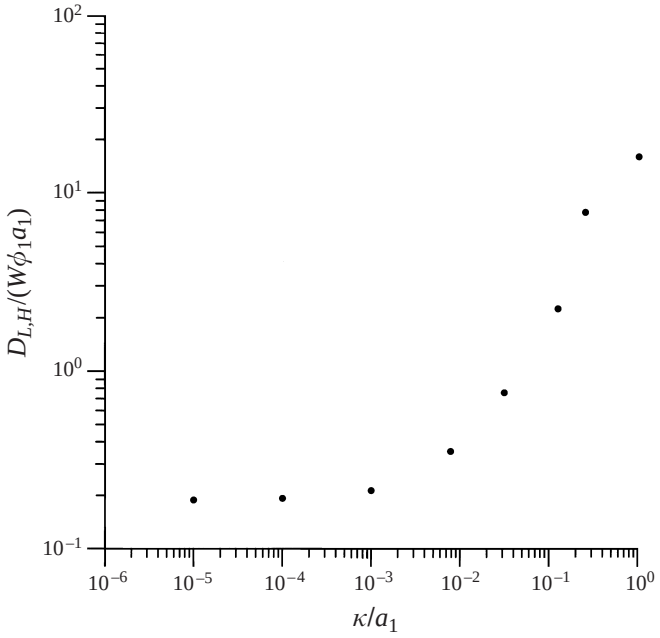

FIGURE 1. The hydrodynamic diffusivity scaled by $Wa_1\phi_1$ is plotted as a function of the ratio of the Brinkman screening length to the sphere radius for relatively impermeable media.

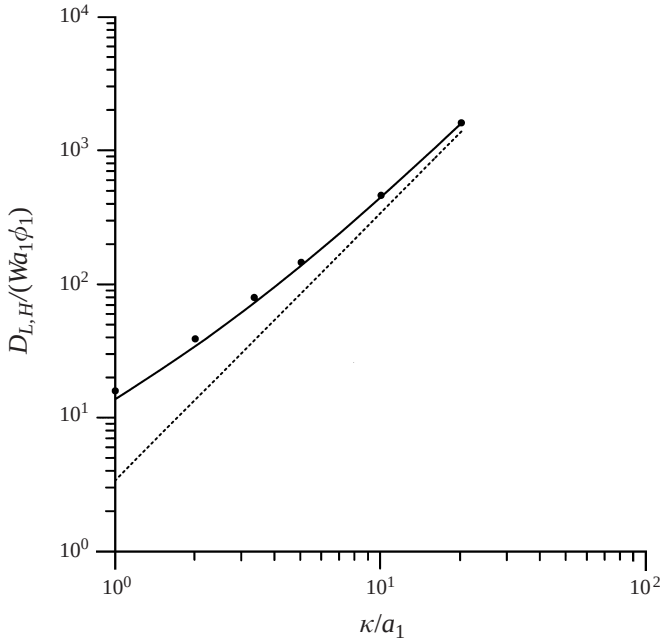

FIGURE 2. The hydrodynamic diffusivity scaled by $Wa_1\phi_1$ (circles) is plotted as a function of the ratio of the Brinkman screening length to the sphere radius for more permeable media. The dashed line is the asymptotic result for $\kappa \gg a_1$ obtained by Koch & Brady (1985) and the solid line is the improved asymptote given by equations (44) and (45).

highly permeable arrays $(27/8)(\kappa/a_1)^2 + 10.34(\kappa/a_1)$ derived in § 3 (equations (44) and (45)) is plotted as the solid line.

2.3. *Boundary-layer dispersion*

The molecular diffusion of the chemical tracer must be included in a description of the dispersion arising from regions close to the particle surface. However, the solution (15) for the fluid velocity can be simplified for $y = r - a_1 \ll \min(a_1, \kappa)$ to take the form

$$\langle u_\theta \rangle_1 = -\frac{3Uy}{2\alpha} \sin\theta, \tag{24}$$

$$\langle u_r \rangle_1 = \frac{3Uy^2}{2a_1\alpha} \cos\theta. \tag{25}$$

Here, u_r and u_θ are the r- and θ-components of the fluid velocity in spherical coordinates and $\alpha^{-1} = a_1^{-1} + \kappa^{-1}$. Substituting (24) and (25) into the equation (9) for the conditional-average velocity and using (5), we obtain at steady state

$$-\frac{3Wy}{2\alpha a_1} \sin\theta \frac{\partial \langle c' \rangle_1}{\partial \theta} + \frac{3Wy^2}{2\alpha a_1} \cos\theta \frac{\partial \langle c' \rangle_1}{\partial y} - \mathrm{D} \frac{\partial^2 \langle c' \rangle_1}{\partial y^2} - \mathrm{D} \frac{1}{a_1^2 \sin\theta} \frac{\partial}{\partial \theta} \left(\sin\theta \frac{\partial \langle c' \rangle_1}{\partial \theta} \right) = W |\nabla \langle c \rangle|. \tag{26}$$

Scaling the radial coordinate $Y = y/\delta$ with the boundary-layer thickness $\delta = a_1 Pe_f^{-1/3}$ and neglecting the small angular diffusion term gives

$$-\tfrac{3}{2} Y \sin\theta \frac{\partial \langle c' \rangle_1}{\partial \theta} + \tfrac{3}{2} Y^2 \cos\theta \frac{\partial \langle c' \rangle_1}{\partial Y} - \frac{\partial^2 \langle c' \rangle_1}{\partial Y^2} = \frac{a_1 \alpha}{\delta} |\nabla \langle c \rangle|, \tag{27}$$

where $Pe_f = W a_1^2/(D\alpha)$. The effect of decreasing the permeability is to increase the velocity gradient near the surface of the particle and thereby decrease the boundary-layer thickness δ. Since the near-surface expansion (24) and (25) of the velocity field is only valid when $\delta \ll \kappa$, the boundary-layer description applies when $Pe \gg a_1^2 \alpha/\kappa^3$, a constraint that becomes more stringent with decreasing permeability. Nonetheless, boundary-layer dispersion will occur at sufficiently high Péclet numbers in any medium. Fortunately, a single scaled partial differential equation (27) can be used to describe the concentration field in the boundary layer for any permeability. The solution of (27) can be expressed as

$$\langle c' \rangle_1 = S \frac{a_1 \alpha}{\delta} |\nabla \langle c \rangle|, \tag{28}$$

where S is the solution of (27) with the right-hand side replaced by 1 subject to the boundary condition $S = 0$ at $\theta = \pi$. The solution for S as $Y \to \infty$ can be obtained by neglecting the molecular diffusion term in (27) and solving using the method of characteristics; this yields

$$S = \frac{2(\pi - \theta)}{3Y \sin\theta} \quad \text{for} \quad Y \gg 1. \tag{29}$$

For $Y = O(1)$, (27) must be solved numerically subject to the boundary conditions $\partial S/\partial \theta = 0$ at $\theta = \pi$, $\partial S/\partial Y = 0$ at $Y = 0$, and S is required to equal the asymptote (29) at $Y = Y_\infty$. The numerical solution was accomplished using the finite control volume method (Patankar 1980) with a piecewise linear radial profile for the diffusive terms and the radial convective term and an upwind difference scheme in the angular

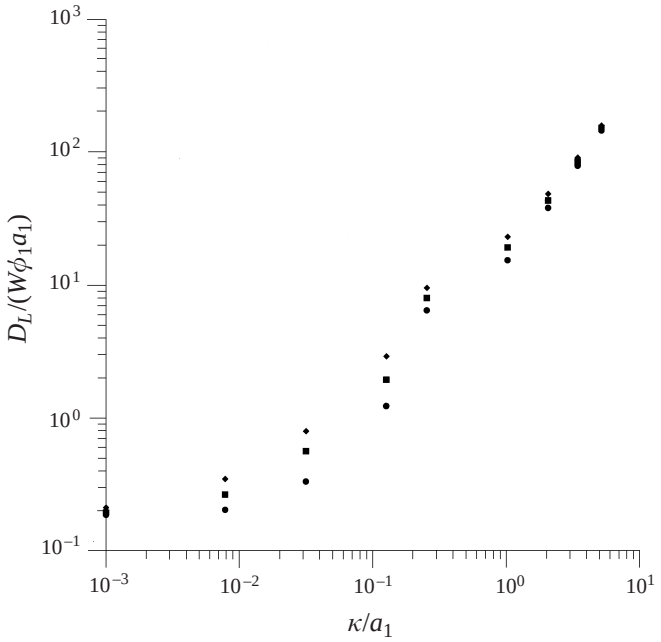

FIGURE 3. The longitudinal diffusivity including both hydrodynamic and boundary-layer dispersion is plotted as a function of permeability, κ/a_1, for three values of the Péclet number based on the large-sphere radius, $Pe_1 = Wa_1/D = 10^2$ (circles), 10^4 (squares), and 10^6 (diamonds).

direction. This yields a set of linear algebraic equations for the concentration at a given angular position when the concentrations at previous values of θ are known; these equations were solved by the tridiagonal-matrix algorithm.

The boundary-layer contribution to the effective diffusivity is obtained by substituting $\langle \boldsymbol{v}' \rangle_1 \approx -\boldsymbol{W}$ and the solution (28) for the concentration field into (6) and integrating over the boundary-layer region $y < \zeta a_1$ or equivalently $Y < Y_m = \zeta a_1/\delta$. We obtain

$$D^*_{L,BL} = \pi^2 \alpha \phi_1 W(\tfrac{1}{6} \ln (Pe_f) + \tfrac{1}{2} \ln \zeta + A), \tag{30}$$

where $\zeta = 0.05$ for $\kappa/a_1 \geqslant 1$, $\zeta = 0.05\kappa/a_1$ for $\kappa/a_1 \leqslant 1$, and

$$A = -\tfrac{1}{2} \ln Y_\infty + \frac{3}{2\pi^2} \int_0^{Y_\infty} \mathrm{d}Y \int_0^{\pi} \sin\theta \, \mathrm{d}\theta \, S = 0.482. \tag{31}$$

Performing the integral in (31) with $Y_\infty = 18$ gives $A = 0.482$; it was determined that this value of Y_∞ was large enough that the overall value of the boundary-layer dispersion contribution was independent of Y_∞.

The boundary-layer dispersion contribution (30) must be added to the hydrodynamic diffusion (22) occurring in the region $Y > \zeta a_1$ to obtain the complete solution for the longitudinal diffusivity for an array of spheres in a Brinkman medium. The relative importance of boundary-layer and hydrodynamic dispersion over a range of values of the ratio of screening length to large particle radius can be seen in figure 3 by comparing the longitudinal diffusivities scaled with $Wa_1\phi_1$ for three different Péclet numbers. The hydrodynamic diffusion yields a contribution to $D_L/(Wa_1\phi_1)$ that is independent of the Péclet number, while the boundary-layer contribution grows logarithmically with Pe. Therefore, the importance of boundary-layer dispersion can be

judged by noting the spread in the values of $D_L/(Wa_1\phi_1)$ for different Péclet numbers. When the permeability is small, the velocity gradients near the surface of the sphere are large and the boundary layer is thin. Thus, boundary-layer dispersion is small in this limit and this justifies its neglect in the analysis of the Darcy flow problem by Moutsopoulos & Bories (1993). When the Brinkman screening length is comparable with the radius of the large particles, boundary-layer dispersion makes a significant contribution to the overall dispersion. As the permeability is increased further, the contribution to the overall diffusion due to the boundary layer near each sphere reaches a finite asymptote, while the hydrodynamic dispersion per particle grows like $(\kappa/a_1)^2$. Thus, hydrodynamic dispersion dominates in the limit of large permeability.

In the foregoing analysis of boundary-layer dispersion, we neglected the hydrodynamic diffusivity produced by the small spheres compared with molecular diffusion. This may seem surprising at first since we are interested in high Péclet numbers where hydrodynamic diffusion is expected to dominate. However, the present analysis is asymptotically valid for the case where the Péclet number for the large spheres is large but that for the small spheres is small, i.e. $Pe = Ua_1/D \gg 1$ and $Pe_2 = Ua_2/D \ll 1$. In addition, it is applicable to dilute arrays, $\phi_2 \ll 1$, with any value of Pe_2.

Koch (1996) showed that hydrodynamic diffusion is suppressed near solid boundaries to a porous medium. In particular the radial component of the diffusivity depends on the time integral of the radial velocity correlation function of a tracer molecule being convected around the circumference of the large sphere and can be estimated as $v_r'^2\tau$ where $\tau = \kappa/v_\theta$ is the correlation time or the time for which the tracer experiences the velocity disturbance of one of the small spheres. The radial velocity disturbance caused by a small sphere, $v_{r'}'$, is proportional to Ua_2Y^2/κ^3 and the tangential velocity sweeping the tracer around the large sphere, v_θ, is proportional to U_Y/α as $y \to 0$. As a result the hydrodynamic diffusion in the boundary layer $Y = O(\delta)$ is $O(Ua_2^2\delta^3\alpha/\kappa^5)$ or $O(Da_2^2/\kappa^2)$. In a dilute array the hydrodynamic diffusivity is thus $O(\phi_2)$ smaller than the molecular diffusivity in the mass-transfer boundary layer. When $\phi_2 = O(1)$, hydrodynamic diffusion and molecular diffusion have the same order of magnitude and the theory provides a qualitatively (but not quantitatively) accurate description of the boundary-layer dispersion.

3. Theory for highly permeable media $k \gg a_1$

In this section, we will consider a dilute, highly permeable fixed bed, in which $a_1/a_2 = O(1)$, and $\phi = \phi_1 + \phi_2 \ll 1$. Each species will then make a significant contribution to the effective diffusivity. Because of the long range of the velocity disturbances in a dilute bed, multiparticle reflections are more important here than for more moderate permeabilities. Thus, we will retain higher-order terms in the expansion (6) for the effective diffusivity. In a highly permeable medium, $\kappa \gg a_1$, the largest contribution to the hydrodynamic diffusivity comes from large $O(\kappa)$ radial distances from the test particle. At these large distances, the velocity disturbance caused by the particle can be approximated using the point-particle approximation. For an array of randomly positioned point particles, the expansion for the effective diffusivity can be written as

$$\boldsymbol{D}^* = \boldsymbol{D}_1^* + \boldsymbol{D}_2^* + \boldsymbol{D}_{11}^* + \boldsymbol{D}_{12}^* + \boldsymbol{D}_{22}^*, \tag{32}$$

where

$$-\boldsymbol{D}_i^* \cdot \nabla\langle c\rangle = n_i\kappa^4 \int \mathrm{d}\boldsymbol{x}_A \langle \boldsymbol{v}'\rangle_1(\boldsymbol{x}|\boldsymbol{x}_A, i)\langle c'\rangle_1(\boldsymbol{x}|\boldsymbol{x}_A, i), \tag{33}$$

$$-\boldsymbol{D}_{ij}^{*}\cdot\nabla\langle c\rangle = n_i n_j \kappa^7 \int \mathrm{d}\boldsymbol{x}_A \mathrm{d}\boldsymbol{x}_B \langle \boldsymbol{v}''\rangle_2(\boldsymbol{x}|\boldsymbol{x}_A, i; \boldsymbol{x}_B, j)\langle c''\rangle_2(\boldsymbol{x}|\boldsymbol{x}_A, i; \boldsymbol{x}_B, j); \tag{34}$$

$\langle\ \rangle_1(\boldsymbol{x}|\boldsymbol{x}_A, i)$ is the conditional average of a property at $\boldsymbol{x}$ when a particle of species i is located at $\boldsymbol{x}_A$, $\langle\ \rangle_2(\boldsymbol{x}|\boldsymbol{x}_A, i; \boldsymbol{x}_B, j)$ is the conditional average for a particle of species i at $\boldsymbol{x}_A$ and one of species j at $\boldsymbol{x}_B$, $\boldsymbol{v}'' = \boldsymbol{v} - \langle\boldsymbol{v}\rangle - \langle\boldsymbol{v}'\rangle_1(\boldsymbol{x}|\boldsymbol{x}_A, i) - \langle\boldsymbol{v}'\rangle_1(\boldsymbol{x}|\boldsymbol{x}_B, j)$, $c'' = c - \langle c\rangle - \langle c'\rangle_1(\boldsymbol{x}|\boldsymbol{x}_A, i) - \langle c'\rangle_1(\boldsymbol{x}|\boldsymbol{x}_B, j)$, and all positions have been non-dimensionalized by κ. With $O(\phi)$ relative errors, we can approximate $\boldsymbol{v}$ by $\boldsymbol{u}$.

The conditional-average velocity disturbance caused by a point particle can be obtained from the general expression (15) for the velocity field by non-dimensionalizing r with κ and taking the limit $a_i \ll \kappa$. Retaining terms up to order $(a_i/\kappa)^2$, we obtain

$$\langle\boldsymbol{u}'\rangle_1(\boldsymbol{r}|\boldsymbol{0}, i) = -6\pi\left(\frac{a_i}{\kappa} + \frac{a_i^2}{\kappa^2}\right)\boldsymbol{U}\cdot\boldsymbol{J}(\boldsymbol{r}), \tag{35}$$

$$\boldsymbol{J} = \frac{\boldsymbol{I}}{4\pi r^3}[(1 + r + r^2)\mathrm{e}^{-r} - 1] + \frac{\boldsymbol{rr}}{4\pi r^5}[3 - (3 + 3r + r^2)\mathrm{e}^{-r}], \tag{36}$$

which corresponds to the velocity field produced by a point force of strength (in dimensional variables) $6\pi\mu a_1 U(1 + a_1/\kappa)$ in a Brinkman medium.

The conditionally averaged concentration field can be determined from (9). The term $\langle\boldsymbol{u}'c'\rangle$ in the unconditionally averaged mass conservation equation has been shown to result in the diffusive flux $-\boldsymbol{D}^{*}\cdot\nabla\langle c\rangle$, cf. (4) and (6). We will adopt the self-consistent approximation that $\langle\boldsymbol{u}''c''\rangle_1 - \langle\boldsymbol{u}'c'\rangle$ in the conditional-average mass conservation equation is equal to $-\boldsymbol{D}^{*}\cdot\nabla\langle c'\rangle_1$. Neglecting molecular diffusion, considering the steady-state concentration disturbance caused by the particle, and scaling positions with κ, (9) becomes

$$\frac{\partial\langle c'\rangle_1}{\partial z} = -\langle\boldsymbol{u}'\rangle_1\cdot\nabla\langle c\rangle - \langle\boldsymbol{u}'\rangle_1\cdot\nabla\langle c'\rangle_1 + \frac{1}{\kappa}\nabla\cdot[\boldsymbol{D}^{*}\cdot\nabla\langle c'\rangle_1]. \tag{37}$$

The fluid velocity disturbance $\langle\boldsymbol{u}'\rangle_1$ produced by the particles is small, $O(Ua_i/\kappa)$, and the effective diffusivity is small, $O(Ua_i)$ so that the last two terms on the right-hand side of (37) are $O(a_i/\kappa)$ smaller than the bulk convection term on the right-hand side. Thus, we can expand the concentration field

$$\langle c'\rangle_1 = c_0 + c_1 + \ldots, \tag{38}$$

where

$$\frac{\partial c_0}{\partial z} = -\langle\boldsymbol{u}'\rangle_1\cdot\nabla\langle c\rangle, \tag{39}$$

$$c_1 = c_D + c_N, \tag{40}$$

and c_N and c_D are the first corrections to the concentration field produced by the nonlinear convection term and by the sampling of the concentration field due to the effective diffusivity. These are given by

$$\frac{\partial c_N}{\partial z} = -\langle\boldsymbol{u}'\rangle_1\cdot\nabla c_0, \tag{41}$$

$$\frac{\partial c_D}{\partial z} = \frac{1}{\kappa}\nabla\cdot[\boldsymbol{D}^{*}\cdot\nabla c_0]. \tag{42}$$

The one-particle contribution to the diffusivity $\boldsymbol{D}_i^{*}$ can be expressed as a sum of contributions:

$$\boldsymbol{D}_i^{*} = \boldsymbol{D}_{i,0}^{*} + \boldsymbol{D}_{i,N}^{*} + \boldsymbol{D}_{i,D}^{*} + \ldots \tag{43}$$

obtained by inserting c_0, c_N, c_D, etc, into (33).

The leading-order contribution $\boldsymbol{D}^*_{i,0}$ is identical to that calculated by Koch & Brady (1985). The calculation is done most easily by integrating over z by parts and then taking the Fourier transform in the plane perpendicular to the mean velocity. The result is

$$\boldsymbol{D}^*_{i,0} = \tfrac{27}{8} U a_i \phi_i \left(\frac{\kappa^2}{a_i^2} + \frac{2\kappa}{a_i} \right) \boldsymbol{e}_z \boldsymbol{e}_z. \tag{44}$$

To leading order in small a_i/κ (or equivalently small ϕ), we can superimpose the velocity disturbances caused by the two types of particles (44) as calculated by Koch & Brady (1985). However, these contributions are coupled through the permeability, which depends on the concentrations and radii of both species.

To determine the first influence of the nonlinear convection term on the effective diffusivity, we require a four-dimensional numerical integration. One integral over z is required to determine c_0 from (39) followed by a second integral over z to find c_N from (41). Exploiting axisymmetry, the volume integral in (33) can be reduced to a two-dimensional numerical integration. The result is

$$\boldsymbol{D}^*_{i,N} = 3.59 \; U a_i \phi_i \frac{\kappa}{a_i} \boldsymbol{e}_z \boldsymbol{e}_z. \tag{45}$$

The sum of the terms (44) and (45) provides the improved asymptote for high permeability that is plotted as the dashed line in figure 2.

The fore–aft symmetry of the flow around a single particle in an isotropic Brinkman medium implies that the hydrodynamic diffusivity will be purely longitudinal as obtained above in (44) and (45). Contributions to the transverse diffusivity will arise if we consider multiparticle effects on the concentration field, in particular, the sampling of the space surrounding the test particle at position $\boldsymbol{x}_A$ due to the hydrodynamic diffusion caused by all the other particles (leading to $\boldsymbol{D}^*_{i,D}$) and multiparticle velocity disturbances (leading to $\boldsymbol{D}^*_{ij}$).

The contribution of diffusive sampling to the hydrodynamic diffusivity can be derived most easily by using Fourier transforms. Solving (39) and (42) in Fourier space, the concentration disturbance caused by diffusive sampling is

$$\hat{c}_D = \frac{6\pi a_i \boldsymbol{U} \cdot \hat{\boldsymbol{J}}(\boldsymbol{\xi}) \cdot \nabla \langle c \rangle (2\pi)^2 \boldsymbol{\xi} \cdot \boldsymbol{D}^* \cdot \boldsymbol{\xi}}{\kappa (2\pi \xi_z)^2 U^2} \tag{46}$$

where $\boldsymbol{\xi}$ is the Fourier transform variable corresponding to $\boldsymbol{x} - \boldsymbol{x}_A$ and

$$\hat{\boldsymbol{J}}(\boldsymbol{\xi}) = \frac{\boldsymbol{I} - \boldsymbol{\xi}\boldsymbol{\xi}/\xi^2}{(2\pi\xi)^2 + 1} \tag{47}$$

is the Fourier transform of the Green's function for Brinkman's equation. This may be derived most easily by consider Brinkman's equation (12) and (10) with a point-particle forcing $\boldsymbol{F}\delta(\boldsymbol{r})$ on the right-hand side, scaling the position variable, Fourier transforming, solving for $\langle \hat{\boldsymbol{u}}' \rangle_1$, and using (35).

Substituting (46) and (35) into (33) and using the product theorem we obtain an expression for the effects of diffusive sampling on the effective diffusivity:

$$\boldsymbol{D}^*_{i,0} = n_i \kappa (6\pi a_i)^2 \int \mathrm{d}\boldsymbol{\xi} \frac{\boldsymbol{e}_z \cdot \hat{\boldsymbol{J}}(\boldsymbol{\xi}) \boldsymbol{e}_z \cdot \hat{\boldsymbol{J}}(-\boldsymbol{\xi}) \boldsymbol{\xi} \cdot \boldsymbol{D}^* \cdot \boldsymbol{\xi}}{(2\pi\xi_z)^2} \tag{48}$$

Using the leading-order estimate for the effective diffusivity

$$\boldsymbol{D}^* \approx \boldsymbol{D}^*_{10} + \boldsymbol{D}^*_{20} \approx \boldsymbol{e}_z \boldsymbol{e}_z \tfrac{27}{8} U \kappa^2 \left(\frac{\phi_1}{a_1} + \frac{\phi_2}{a_2} \right) \tag{49}$$

in the integral on the right-hand side of (48), we obtain

$$\boldsymbol{D}^*_{i,D} = \frac{243\pi^2}{2} n_i U \kappa^3 a_i^2 \left(\frac{\phi_1}{a_1} + \frac{\phi_2}{a_2}\right) \int \mathrm{d}\boldsymbol{\xi} \boldsymbol{e}_z \cdot \hat{\boldsymbol{J}}(\boldsymbol{\xi}) \boldsymbol{e}_z \cdot \hat{\boldsymbol{J}}(-\boldsymbol{\xi}) \tag{50}$$

or

$$\boldsymbol{D}^*_{i,D} = \left(\frac{243}{40}\boldsymbol{e}_z\boldsymbol{e}_z + \frac{243}{320}(\boldsymbol{I} - \boldsymbol{e}_z\boldsymbol{e}_z)\right) \phi_i U \frac{\kappa^3}{a_i} \left(\frac{\phi_1}{a_1} + \frac{\phi_2}{a_2}\right), \tag{51}$$

Koch & Brady (1985) studied the effects of diffusive sampling on the transverse effective diffusivity in monodisperse fixed bed. They obtained an $O(Ua\phi^{1/2})$ transverse diffusivity consistent with (51). However, an algebraic error in Koch & Brady's analysis led to an incorrect numerical coefficient in their equation (4.11).

Next, we consider the contribution of two-particle velocity correlations to the effective diffusivity, i.e, $\boldsymbol{D}^*_{ij}$ defined by (34). The velocity disturbance produced by a particle is weak, $O(Ua_i/\kappa)$ at $O(\kappa)$ separations. As a result, each successive, higher-order hydrodynamic reflection between two particles is $O(a_i/\kappa)$ smaller than the preceding one. The leading-order two-particle velocity disturbance involves first reflections. The fluid velocity disturbance $6\pi(a_i/\kappa)\boldsymbol{U} \cdot \boldsymbol{J}(\boldsymbol{x}_B - \boldsymbol{x}_A)$ produced by particle A modifies the force on particle B and the disturbance $6\pi(a_j/\kappa)\boldsymbol{U} \cdot \boldsymbol{J}(\boldsymbol{x}_A - \boldsymbol{x}_B)$ produced by B modifies the force on A. These modified forces produce the velocity field

$$\langle \boldsymbol{u}'' \rangle_2 = (6\pi)^2 \frac{a_i a_j}{\kappa^2} [\boldsymbol{U} \cdot \boldsymbol{J}(\boldsymbol{x}_B - \boldsymbol{x}_A) \cdot \boldsymbol{J}(\boldsymbol{x} - \boldsymbol{x}_B) + \boldsymbol{U} \cdot \boldsymbol{J}(\boldsymbol{x}_A - \boldsymbol{x}_B) \cdot \boldsymbol{J}(\boldsymbol{x} - \boldsymbol{x}_A)]. \tag{52}$$

An equation for the two-particle concentration disturbance $\langle c'' \rangle_2$ similar to (9) for the one-particle disturbance can be derived by taking the average of (3) with two particle positions held fixed and subtracting the bulk average mass conservation equation (4) and equations of the form (9) for the disturbances due to each of the two particles. To leading order in small volume fraction, the resulting equation reduces to

$$\boldsymbol{U} \cdot \nabla \langle c'' \rangle_2 \approx -\langle \boldsymbol{u}'' \rangle_2 \cdot \nabla \langle c \rangle. \tag{53}$$

Introducing inverse Fourier transformer for the Green's functions in (52), solving (53) in Fourier space and inserting the resulting expressions into (34) gives

$$\boldsymbol{D}^*_{ij} = (6\pi)^4 n_i n_j \kappa^2 a_i^2 a_j^2 \, \mathrm{U} \, \boldsymbol{B}, \tag{54}$$

where

$$B_{ij} = \int \mathrm{d}\boldsymbol{\xi} \frac{\delta_{k3}\delta_{m3}}{2\pi i \xi_3} \hat{J}_{li}(\boldsymbol{\xi}) \hat{J}_{nj}(\xi) A_{klmn} \tag{55}$$

and

$$A_{klmn} = \int \mathrm{d}\boldsymbol{\xi}' \hat{J}_{kl}(\boldsymbol{\xi}') \hat{J}_{mn}(\boldsymbol{\xi}'). \tag{56}$$

In (55) and (56), we have adopted index notation and δ_{k3} is the unit vector parallel to the mean velocity. Performing the integrals in (56) gives

$$A_{klmn} = \frac{1}{8\pi}(\tfrac{2}{5}\delta_{kl}\delta_{mn} + \tfrac{1}{15}(\delta_{mk}\delta_{ln} + \delta_{kn}\delta_{lm})). \tag{57}$$

Substituting (57) into (55), interpreting $1/\xi_3$ as a generalized function and performing the integration over $\boldsymbol{\xi}$, we obtain

$$\boldsymbol{B} = \frac{1}{128\pi^2}(\boldsymbol{e}_z\boldsymbol{e}_z + \tfrac{1}{15}\boldsymbol{I}). \tag{58}$$

Thus, the effective diffusivity due to two-particle interactions is

$$\boldsymbol{D}_{ij}^{*} = \left(\frac{243}{40} \boldsymbol{e}_z \boldsymbol{e}_z + \frac{243}{640} (\boldsymbol{I} - \boldsymbol{e}_z \boldsymbol{e}_z) \right) \phi_i \phi_j U \frac{\kappa^3}{a_i a_j}. \tag{59}$$

Because the streamlines for flow past two interacting particles in a Brinkman medium do not have fore–aft symmetry, $\boldsymbol{D}_{ij}^{*}$ includes a contribution to the transverse as well as the longitudinal diffusivity. The effects of two-particle interactions on the transverse stretch of a polymer molecule in a fixed bed of spheres has been analysed by Shaqfeh & Koch (1992).

To obtain results for the diffusivity in terms of the particle volume fractions and radii alone, we must relate the permeability to ϕ_1, ϕ_2, a_1, and a_2. The body force that the particles exert on the fluid is

$$-\mu U/\kappa^2 = n_1 F_1 + n_2 F_2. \tag{60}$$

Here, F_1 is the average force that each particle exerts, which can be obtained from a solution for flow past a sphere in a Brinkman medium:

$$F_i = -6\pi\mu U a_i \left(1 + a_i/\kappa\right). \tag{61}$$

Gathering together the various contributions (44), (45), (51), and (59) to the hydrodynamic diffusivity along with the boundary-layer diffusivity (32), the longitudinal and transverse effective diffusivities in a dilute bidisperse fixed bed are given by

$$\begin{aligned} D_L^{*} = U a_1 \Bigg(& \frac{3}{4} \left(1 + \frac{f}{\lambda}\right) \left(1 + \frac{f}{\lambda^2}\right)^{-1} - \frac{9\phi_1^{1/2}}{20(2)^{1/2}} \left(1 + \frac{f}{\lambda}\right)^2 \left(1 + \frac{f}{\lambda^2}\right)^{-3/2} \\ & + 4.87\phi_1^{1/2}(1+f) \left(1 + \frac{f}{\lambda^2}\right)^{-1/2} + \frac{\pi^2}{6}\phi_1 [\ln(Pe) + f\lambda \ln(\lambda Pe)] \\ & + O\left(\phi_1 [\ln(1/\phi_1)]^2\right) \Bigg), \end{aligned} \tag{62}$$

$$D_T^{*} = U a_1 \left(\frac{27}{160\sqrt{2}} \phi_1^{1/2} \left(1 + \frac{f}{\lambda}\right)^2 \left(1 + \frac{f}{\lambda^2}\right)^{-3/2} + O(\phi_1) \right), \tag{63}$$

where $f = \phi_2/\phi_1$ and $\lambda = a_2/a_1$.

For a monodisperse fixed bed (62) becomes

$$D_L^{*} = U a_1 \left(\tfrac{3}{4} + 4.55\phi_1^{1/2} + \tfrac{1}{6}\pi^2 \phi \ln(Pe) + O(\phi_1 [\ln(1/\phi_1)]^2) \right). \tag{64}$$

The first and third terms in the brackets on the right-hand side of (64) are the hydrodynamic and boundary-layer dispersion contributions derived by Koch & Brady (1985), while the second term represents the first correction to Koch & Brady's hydrodynamic diffusion result due to effects of diffusive sampling, two-particle interactions, the nonlinear convective term in the mass conservation equation, and corrections to the particle force and permeability. The next, $O(\phi_1 [\ln(1/\phi_1)]^2)$ correction to D_L^{*} comes from the second perturbation of the concentration field by the nonlinear convective term in (37). The transverse diffusivity in a monodisperse fixed bed obtained by setting $f = 0$ in (63) is

$$D_T^{*} = U a_1 \left(\frac{27}{160\sqrt{2}} \phi_1^{1/2} + O(\phi_1) \right). \tag{65}$$

This transverse dispersion coefficient contains contributions due to both diffusive

sampling as noted by Koch & Brady (1985) and two-particle interactions as suggested (in a slightly different context) by Shaqfeh & Koch (1992).

4. Experimental study of dispersion in a bidisperse packed bed

The approximations used in the foregoing analysis are asymptotically valid in the dilute limit, $\phi_1 \ll 1$ and $\phi_2 \ll 1$. When $\phi_2 \sim O(1)$, Brinkman's equations of motion will no longer describe the detailed conditional-average velocity profile around a test (species 1) sphere (Durlofsky & Brady 1987). However, based on the success of theories using Brinkman's equation to predict average properties of concentrated fixed beds (Koch & Brady 1985; Sangani & Behl 1989; Koch & Ladd 1997), we might expect the qualitative predictions of the theory to apply to packed beds with $\phi_1 \ll 1$ but $\phi_2 \sim O(1)$.

To explore the behaviour of such packed beds, an experimental study of the dispersion resulting from flow through a bidisperse bed consisting of Fontainebleau sand grains ($a_2 = 102.5\,\mu\text{m}$) and glass spheres (a_1=5 mm) was performed. The bed was contained in a vertical tube of 25 cm diameter and 50 cm height.

When producing a bidisperse packed bed, care must be taken to ensure that there are no macroscopic inhomogeneities due to segregation of the two species or variations in the packing density. The variations in permeability resulting from such inhomogeneities could lead to much higher effective diffusivities than would occur in a statistically homogeneous medium. To ensure a homogeneous medium, the bed was constructed by successively depositing layers of 2 cm thickness and compacting the medium with a cylindrical piston until the porosity reached its minimum value. Media were constructed with $\phi_1 = 0$ and 0.15. In each case, the porosity of the medium consisting of the small spheres, i.e. $(1 - \phi_1 - \phi_2)/(1 - \phi_1)$, was 0.37.

The fluid phase for the dispersion experiments consisted of an aqueous solution of $CaNO_3$. To ensure that the bed was completely saturated with water, the bed was purged with CO_2, which is soluble in both air and water, before introducing the water flow. Experiments were performed at small velocities so that the Reynolds number was in the range $Re = Ua_2/\nu = 0.079$–0.79 where ν is the kinematic viscosity of the water. The relationship between head loss and volumetric flow rate for all three media was linear, indicating a viscous-dominated flow. The permeability of the monodisperse bed, $k_2 = 1.91 \times 10^{-7}\text{cm}^2$, was comparable with the value, $k_2 = 2.98 \times 10^{-7}\text{cm}^2$, predicted by the Carman–Kozeny correlation for spherical particles. The spatial uniformity of the mean flow profile produced by the fluid injection system was verified in a prototype bed containing an array of thermocouples. The temperature of the fluid was changed abruptly and the thermocouples indicated that the temperature profile within the bed was nearly independent of position in the plane perpendicular to the tube axis.

To measure the dispersion, a step change in the inlet concentration of $CaNO_3$ from 1.0 mg l^{-1} to 1.5 mg l^{-1} was introduced into the bottom of the bed. The conductivity and temperature of the solution as a function of time were monitored at the inlet and outlet. The concentration of the tracer could be determined from the conductivity after correcting for any changes resulting from inadvertent temperature fluctuations. The concentration profiles were fitted using a solution of the convection–diffusion equation. This fit was very good in both the bidisperse and monodisperse beds, indicating that the bed was sufficiently long to yield the long-time diffusive behaviour. More details of the experimental procedure are given by Moutsopoulos (1993).

The resulting experimental measurements of the effective diffusivities are plotted as a function of Péclet number, $Pe_1 = Wa_1/D$ in figure 4. The circles are values

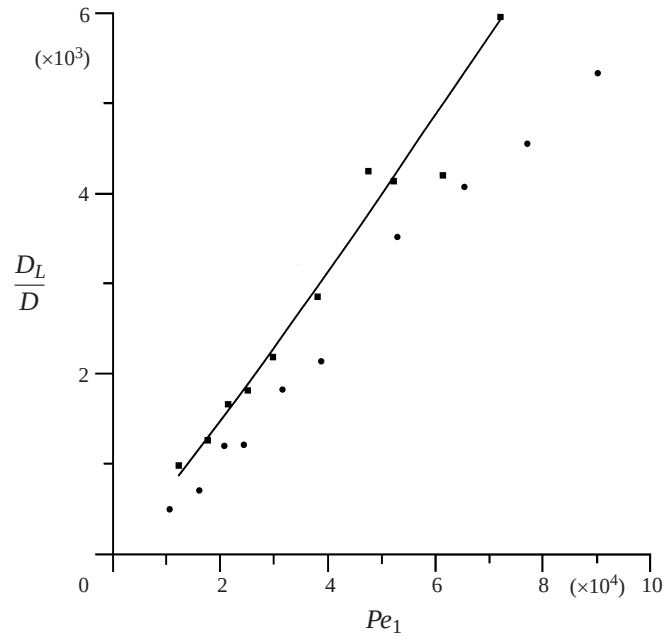

FIGURE 4. Experimental measurements for the logitudinal effective diffusivity non-dimensionalized by the molecular diffusion D are plotted as a function of the Péclet number, $Pe_1 = Wa_1/D$. The squares are experimental results for $\phi_1 = 0.15$ and $a_1/a_2 = 48$ and the line is the corresponding theoretical prediction. For reference the experimental measurements of the effective diffusivity in a monodisperse bed consisting of the small spheres are indicated by the circles.

for a monodisperse bed of small spheres (with radii a_2) and the squares are the measurements for a bidisperse medium with $\phi_1 = 0.15$. The inclusion of large spheres in the medium increases the effective diffusivity substantially above the values obtained in a monodisperse bed even at this relatively modest value of ϕ_1.

To predict the effective diffusivities arising in the bidisperse bed, we will assume that the dispersion resulting from the small and large spheres can be superimposed, $D^* = D_1^* + D_2^*$. As noted above, this superposition strictly holds when $\phi_1(\kappa/a_1)^3 \ll 1$. The dispersion caused by the small spheres is taken to be $D_2^* = (1 - \phi_1)D_M^*$, where D_M^* is the effective diffusivity in a monodisperse bed. A best fit to the data for the monodisperse beds yields $D_M^* = 1.03(Wa_2/D)^{1.145}$. The dispersion D_1^* caused by the large spheres is obtained using the theory derived in § 2, i.e. equations (22) and (30). The permeability k_2 of the medium of small spheres is obtained from the Carman–Kozeny correlation. The resulting theoretical predictions are shown as the solid line in figure 4. The theory and experiment are in good agreement in terms of both the magnitude of the enhancement of dispersion and its dependence on Péclet number. The theory indicates that the enhancement of dispersion due to the large spheres is nearly entirely a result of hydrodynamic dispersion with very little boundary-layer dispersion as one might expect for a medium with such a large size ratio, $a_1/a_2 = 48$.

The only previous experimental study of dispersion in an unconsolidated bidisperse packed bed in the literature is that of Lemaitre *et al.* (1986). These authors considered particles with a size ratio, $a_1/a_2 = 10$. The main goal of their study was to observe the very large enhancement of dispersion that they argued would occur when the large spheres were sufficiently concentrated to create a percolating network of preferential paths for the fluid flow. Experiments were also performed at lower concentrations $\phi_1 =$

0.15 and 0.214. However, the dispersion measured for these cases was approximately eight times higher than our theoretical predictions. In view of the good comparison between our theory and the present experiments, we believe that this large dispersion may have resulted from bed inhomogeneities. This hypothesis is supported by the non-Fickian nature of the concentration profiles measured by Lemaitre *et al.* As noted above, special precautions are necessary to produce a homogeneous bidisperse bed. Hulin *et al.* (1988) and Guyon, Oger & Plona (1987) have also noted the difficulty of producing a homogeneous bidisperse porous medium and have suggested procedures for constructing homogeneous unconsolidated and consolidated media. Hulin *et al.* (1988) obtained experimental measurements of the hydrodynamic diffusivity in consolidated porous media formed by sintering bidisperse packed beds with a particle radius ratio of 3.4. These authors showed that an empirical correlation relating the hydrodynamic diffusivity to the prermeability and conductivity of the medium and the loss of porosity during sintering provided a good fit to their data and to previous data on consolidated media formed from monodisperse packings. However, it is clear that such a correlation could not account for the present experimental observations. For the large radius ratio (48.8) used in our experiments, the effect of the volume fraction of the large spheres on the permeability, porosity and conductivity is small whereas its effect on the hydrodynamic diffusion is substantial.

5. Conclusions

The effective diffusivity due to flow through a bidisperse porous medium has been analysed. The case in which the particles of species 1 are much larger than those of species 2, $a_1/a_2 \gg 1$, is treated in § 2. The permeability of the medium is controlled primarily by the smaller particles, whereas the hydrodynamic diffusion results from the larger particles. The mechanical and boundary-layer dispersion mechanisms identified by Koch & Brady (1985) for a monodisperse fixed bed are found to exist in a bidisperse bed as well. The bidisperse medium can exhibit arbitrary values of the ratio κ/a_1 where κ is the Brinkman screening length or square root of the permeability. Thus, it is necessary to relax Koch & Brady's assumption that most of the hydrodynamic dispersion would occur at large distances from the sphere where the streamlines are nearly straight and instead integrate over the curved streamlines for Brinkman flow past a finite-radius particle. While dispersion is independent of molecular diffusion throughout most of the medium, it is necessary to account for molecular diffusion in a thin mass-transfer boundary layer near each particle's surface. The resulting boundary-layer dispersion constitutes an important contribution to the effective diffusivity when $\kappa = O(a_1)$. However, the size of the boundary-layer dispersion contribution diminishes as $\kappa/a_1 \to 0$. Thus, the results of Moutsopoulos & Bories (1993) for dispersion in a Darcy medium where no boundary layer exists are recovered in this limit.

In § 3, we considered a dilute fixed bed in which $\kappa \gg a_1$. In this section, the ratio of the particle radii was allowed to be $O(1)$ so that each species made a significant contribution to both the permeability and the dispersion. Koch & Brady (1985) showed that the leading-order longitudinal hydrodynamic diffusivity is $(3/4)Ua_1$ in a dilute monodisperse bed. The corresponding result for a bidisperse medium is $(3/4)Ua_1(1 + f/\lambda)(1 + f/\lambda^2)^{-1}$, where $f = \phi_2/\phi_1$ and $\lambda = a_2/a_1$. The longitudinal and transverse hydrodynamic diffusivities were computed including terms up to $O(Ua_1\phi_1^{1/2})$. Corrections of this order arose due to changes in the drag and permeability resulting from particle interactions, the sampling of the space surrounding the test particle due to the effective diffusivity caused by the other particles, the nonlinear

convective term in the mass conservation equation, and the dispersion resulting from fluid velocity disturbances associated with two-particle reflections. In the case of a monodisperse fixed bed, our analysis provides an extension of Koch & Brady's (1985) analysis to include one higher-order term in the expansion for small volume fraction.

Experimental results for the effective diffusivity in a bidisperse bed were presented in § 4. The experiments confirm the theoretical prediction that the dispersion grows upon the inclusion of large spheres in a packed bed of small spheres. Good quantitative agreement between theoretical predictions and experimental measurements of this added dispersion is obtained when the flow around the large spheres is modelled using Brinkman's equation with a permeability obtained from the Carman–Kozeny equation.

The authors thank S. Bories, E. C. Aifantis, C. Tzimopoulos, and E. S. G. Shaqfeh for useful discussions and encouragement. D. L. K. acknowledges financial support from the National Science Foundation grant CTS-9526149.

REFERENCES

Acrivos, A. & Chang, E. 1986 A model for estimating transport quantities in two-phase materials. *Phys. Fluids* **29**, 3.

Aifantis, E. C. 1980 On the problem of diffusion in solids. *Acta Mechanica* **37**, 265.

Bear, J. 1978 Relations between microscopic and macroscopic descriptions in porous media. In *Symp. on the Scale Effects in Porous Media* (ed. J. Ganoulis). Thessaloniki.

Brenner, H. 1980 Dispersion resulting from flow through spatially periodic porous media. *Phil. Trans. R. Soc. Lond.* A **297**, 81.

Brinkman, H. C. 1947 A calculation of the viscous force exerted by a flowing fluid on a dense swarm of particles. *Appl. Sci. Res.* **1**, 27.

Durlofsky, L. & Brady, J. F. 1987 Analysis of the Brinkman equation as a model for flow in porous media. *Phys. Fluids* **30**, 3329.

Eidsath, A., Carbonell, R. G., Whitaker, S. & Herman, L. R. 1983 Dispersion in pulsed systems. III: Comparison between theory and experiments for packed beds. *Chem. Engng. Sci.* **38**, 1803.

Fried, J. J. & Combarnous, M. A. 1971 Dispersion in porous media. *Adv. Hydrosci.* **7**, 169.

Guyon, E., Oger, L. & Plona, T. J. 1987 Transport properties in sintered porous media composed of two particle sizes. *J. Phys.* D **20**, 1637.

Hinch, E. J. 1977 An averaged-equation approach to particle interactions in a fluid suspension. *J. Fluid Mech.* **83**, 695.

Hulin, J. P., Charlaix, E., Plona, T. J., Oger, L. & Guyon, E. 1988 Tracer dispersion in sintered glass beads with a bidisperse size distribution. *AIChE J.* **34**, 610.

Koch, D. L. 1996 Hydrodynamic diffusion near solid boundaries with applications to heat and mass transfer into sheared suspensions and fixed-fibre beds. *J. Fluid Mech.* **318**, 31.

Koch, D. L. & Brady, J. F. 1985 Dispersion in fixed beds. *J. Fluid Mech.* **154**, 399.

Koch D. L. & Brady, J. F. 1988 Anomalous diffusion in heterogeneous porous media. *Phys. Fluids* **31**, 965.

Koch, D. L. & Ladd, A. J. C. 1997 Moderate Reynolds number flows through periodic and random arrays of cylinders. *J. Fluid Mech.* **349**, 31.

Koplik, J., Redner, S. & Wilkinson, D. 1988 Transport and dispersion in random networks with percolation disorder. *Phys. Rev.* A **37**, 2619.

Lemaitre, J., Cintre, M., Troadec, J.-P. & Bideau, D. 1986 Dispersion d'un traceur dans un melange binaire de spheres. *C. R. Acad. Sci. Paris* **303**, 1529.

Lenormand, R. & Wang, B. 1995 A stream tube model for miscible flow, part 2. Macrodispersion in porous media with long range correlations. *Transport in Porous Media* **18**, 263.

Moutsopoulos, K. N. 1993 Dispersion en milieux poreux hétérogènes. PhD thesis, Institut National Polytechnique de Toulouse, France.

Moutsopoulos, K. N. & Bories, S. 1993 Dispersion en milieux poreux hétérogènes. *C.R. Acad. Sci. Paris* **316**, 1667.

Muthukumar, M. & Freed, K. F. 1979 On the Stokes problem for a suspension of spheres at nonzero concentrations. II. Calculations for effective medium theory. *J. Chem. Phys.* **70**, 5875.

Patankar, S. V. 1980 *Numerical Heat Transfer and Fluid Flow*. McGraw-Hill.

Saffman, P. G. 1959 A theory of dispersion in porous media. *J. Fluid Mech.* **6**, 321.

Sahimi, M. & Imdakm, A. O. 1988 The effect of morphological disorder on hydrodynamic dispersion in flows through porous media. *J. Phys.* A **21**, 3833.

Salles, J., Thovert, J.-F., Delannay, R., Prevors, L., Auriault, J.-L. & Adler, P. M. 1993 Taylor dispersion in porous media. Determination of the dispersion tensor. *Phys. Fluids* A **5**, 2348.

Sangani, A. S. & Behl, S. 1989 The planar singular solutions of Stokes and Laplace equations and their application to transport processes near porous surfaces. *Phys. Fluids* **31**, 2405.

Shaqfeh, E. S. G. & Koch, D. L. 1992 Polymer stretch in dilute fixed beds of fibers or spheres. *J. Fluid Mech.* **244**, 17.

Smith, L. & Schwartz, F. W. 1980 Mass transport 1. A stochastic analysis of macroscopic dispersion. *Water Resour. Res.* **16**, 303.